Published in final edited form as:
J Immunother. 2010 September ; 33(7): 684–696. doi:10.1097/CJI.0b013e3181e475e9.

Cord Blood Natural Killer Cells Exhibit Impaired Lytic Immunological Synapse Formation That Is Reversed with IL-2 *Ex Vivo* Expansion

Dongxia Xing[1,*], **Alan G. Ramsay**[1,†], **John G. Gribben**[†], **William K. Decker**[*], **Jared K. Burks**[*], **Mark Munsell**[#], **Sufang Li**[*], **Simon N. Robinson**[*], **Hong Yang**[*], **David Steiner**[*], **Nina Shah**[*], **John D. McMannis**[*], **Richard E. Champlin**[*], **Chitra Hosing**[*], **Patrick A. Zweidler-Mckay**[*], **Elizabeth J. Shpall**[*], and **Catherine M. Bollard**[2,‡]

[*]Departments of Stem Cell Transplantation and Cellular Therapy, The University of Texas M. D. Anderson Cancer Center, Unit 65, 1515 Holcombe Blvd., Houston, TX 77303, USA

[#]Department of Biostatistics, The University of Texas M. D. Anderson Cancer Center, Unit 65, 1515 Holcombe Blvd., Houston, TX 77303, USA

[†]Institute of Cancer, Queen Mary University of London, Centre for Medical Oncology, Barts and The London School of Medicine, London, United Kingdom

[‡]Center for Cell and Gene Therapy, Baylor College of Medicine, Houston, Texas 77030, USA

Abstract

Peripheral blood natural killer (NK) cell therapy for acute myeloid leukemia has shown promise in clinical trials after allogeneic stem cell transplantation (SCT). Cord blood (CB) is another potentially rich source of NK cells for adoptive immune therapy after SCT. Tightly regulated receptor signaling between NK cells and susceptible tumor cells is essential for NK cell-mediated cytotoxicity. However, despite expressing normal surface activating and inhibitory NK receptors, CB-derived NK cells have poor cytolytic activity. In this study, we investigate the cellular mechanism and demonstrate that unmanipulated CB-NK cells exhibit an impaired ability to form F-actin immunological synapses with target leukemia cells compared with peripheral blood-derived NK cells. In addition, there was reduced recruitment of the activating receptor CD2, integrin LFA-1, and the cytolytic molecule perforin to the CB-NK synapse site. *Ex vivo* IL-2 expansion of CB-NK cells enhanced lytic synapse formation including CD2 and LFA-1 polarization and activity. Furthermore, the acquired anti-leukemic function of IL-2-expanded CB-NK cells was validated using a NOD-SCID-IL2Rγ^{null} mouse model. We believe our results provide important mechanistic insights for the potential use of IL-2-expanded CB-derived NK cells for adoptive immune therapy in leukemia.

Introduction

Natural killer (NK) cells play a critical role in the innate immune system (1, 2). These cells recognize and kill virus-infected cells or transformed malignant cells, while recruiting additional immune responses through the secretion of cytokines, including interferon-g (3).

[2]Address correspondence to Catherine Bollard, M.D., Center for Cell and Gene Therapy, Baylor College of Medicine, Houston, Texas 77030, USA. cmbollar@txccc.org Tel: office 832-824-4781.
[1]These authors contributed equally to this work.

Financial Disclosure: All authors have declared there are no financial conflicts of interest in regards to this work.

Thus NK-mediated tumor surveillance represents an important cancer immunotherapeutic strategy.

NK cell-mediated cytotoxicity is regulated by inhibitory NK receptors for MHC class I molecules, including the human killer Ig-like receptors (KIRs) and the heterodimeric C-type lectin receptor (4, 5). In addition, lytic NK cell recognition and function are controlled by activating receptors, such as NKG2D or natural cytotoxicity receptors (NCRs). Three NCRs have been described: NKp46, NKp30, and NKp44. NKp46 and NKp30 are constitutively expressed on all peripheral blood (PB) NK cells (6), whereas NKp44 is expressed only on IL-2-activated PB-NK cells (7). Killing of tumor cells occurs when the usually dominant inhibitory interactions between MHC-I molecules expressed on the tumor cells and inhibitory NK receptors are either absent or weak, leading to NCR activation and NK lytic activity.

Alloreactive NK cell-mediated killing has shown significant immunotherapeutic promise in patients with acute myeloid leukemia (AML) following transplantation of allogeneic PB-derived hematopoietic stem cells or the adoptive transfer of alloreactive NK cells (8-10). However, a significant proportion of leukemia patients, especially non-Caucasians, lack a suitable transplant donor. Umbilical cord blood (CB) represents a critical alternative source of stem cells for allotransplant patients. Advantages include the requirement for less stringent HLA matching due to a relatively low risk of graft-versus-host disease compared with bone marrow and PB allografts (11). A recent study has demonstrated decreased relapse rates and improved leukemia-free survival after KIR-ligand mismatched CB transplantation for AML (12). Adoptive transfer of CB-NK cells therefore represents an attractive immunotherapeutic strategy that could be used in combination with CB transplantation in an attempt to enhance anti-leukemia responses, particularly for tackling minimal residual disease. However, it is well established that the cytolytic function of unmanipulated CB-NK cells is weak that may reduce the NK anti-tumor response (13, 14). Thus, understanding the cellular mechanism of suppressed cytolytic CB-NK cell activity and identifying *ex vivo* expansion strategies should facilitate the use of activated CB-NK cells for adoptive immunotherapy treatment strategies in AML.

We hypothesized that CB-NK cells would be ineffective in their ability to functionally interact with target cells. The cytolytic effector function of NK cells requires tightly regulated signaling. Specifically, NK cell contact with a target cell (conjugate interaction) is required with formation of the F-actin NK cell immunological synapse, which is a dynamic signaling interface mediating delivery of lytic granules by directed secretion (15,16). The formation of a mature and functional NK cell lytic synapse has three phases: initiation, effector, and termination. The initiation stage establishes direct cell-cell contact of the NK cell to its target cell through the recruitment and activity of the CD2 receptor (17), integrins such as LFA-1 (18), and natural cytotoxicity receptors (NCRs) (19). In addition, KIR receptors regulate inhibitory synapses to ensure that only ‘foreign’ cells are killed by NK cell lytic synapses. Effective target cell recognition results in NK cell F-actin cytoskeleton reorganization and formation of the mature effector immune synapse that includes recruitment of perforin-rich lytic granules to the synapse site (16, 20). The termination stage occurs after lytic-granule contents have been secreted into the target cell via the synapse and involves synapse molecule down-modulation (21).

In this study, we determined that unmanipulated CB-NK cells are ineffective in forming F-actin immunological synapses with AML target cells compared with PB-NK cells. This was associated with reduced recruitment of key signaling molecules that regulate the formation of the mature lytic synapse, including CD2, LFA-1, and perforin. Critically, we show that *ex vivo* IL-2 expansion of CB-NK cells enhanced lytic synapse formation with CD2 and LFA-1

polarization and adhesive activity. Moreover, we demonstrate *in vivo* anti-leukemia activity of IL-2-expanded CB-NK cells using a NOD-SCID-IL2Rγ^{null} mouse model. Our results indicate that adoptive transfer of IL-2-expanded functional CB-NK cells may have potential clinical application for patients with AML.

Materials and Methods

Patients and Cell preparation

CB and PB samples were obtained fresh from healthy donors who gave informed consent under M. D. Anderson Cancer Center protocols Lab03-0976 (CB) and Lab02-0630 (PB). Frozen apheresis samples were obtained from 12 AML patients. Mononuclear cells were isolated by Ficoll density gradient centrifugation.

(i)Isolation and expansion of CB-derived and PB-derived NK cells—Positive selection of CD56$^+$ CD3$^-$ cells was performed by immunomagnetic separation according to the manufacturer's instructions (Miltenyi Biotech). After selection, the purity of the CD56$^+$CD3$^-$ cells was >96%. Freshly isolated CB-NK cells or PB-NK cell were plated in a T-25 flask at 1×10^6/ml and expanded ex vivo for 14 days in RPMI-1640 medium supplemented with 10% AB human serum (Atlanta Biologicals) and IL-2 (Proleukin; Chiron). The IL-2 was replenished every 3 days to a final concentration of 500 IU/ml. Flow cytometric analysis was performed before and after expansion.

(ii) Isolation of AML blasts—AML blasts were purified by lineage depletion using CD3, CD19, and CD56 antibodies. Flow cytometry demonstrated the purified AML blasts to be CD3$^-$, CD19$^-$, CD56$^-$, and CD45$^+$CD33$^+$CD11b$^+$. AML blasts were used as targets in interferon-γ ELISpots, cytotoxicity assays (including *in vivo* work), and synapse assays.

Phenotyping using flow cytometry

The following monoclonal mAbs from BD Biosciences were used for flow cytometric analysis: anti-CD3 Per CP, anti-CD158a PE (HP-3E4), CD158b PE (CH-L), anti-CD94 PE, anti-NKp30 PE (P30-15), anti-NKp44 PE (P44-8.1), anti-NKp46 PE (9E2), and CD56 APC (NCAM16.2). Flow analysis was performed analyzed by FACSCalibur using CellQuest Pro software (BD Biosciences).

NK cell cytotoxicity assay

Serial dilutions of NK cells were mixed in triplicate for 4 h with 5000 ^{51}Cr-labeled target cells (Amersham Pharmacia Biotech) in a V-bottom 96-well plate (Costar). Targets consisted of K562 cells (American Type Culture Collection) or patient AML blasts. At the end of a 4-h incubation period, supernatants were harvested, and ^{51}Cr release was measured on a microplate scintillation and luminescence counter (TOPCount NXT, Perkin-Elmer). Human B-lymphoblastoid cell line Daudi was used as a negative control. Specific lysis was determined by the formula: specific lysis = (sample value – spontaneous lysis)/(max lysis – spontaneous lysis) × 100%.

IFN-g ELISPOT

The IFN-g ELISPOT assay was performed using unmanipulated and expanded CB-NK and PB-NK cells. NK cells (2 × 10^5) and target cells (K562, primary AML blasts, or control Daudi cells 10^4) were plated onto anti-IFN-γ coated ELISpot plates. IFN-γ spots were developed using a human IFN-γ kit (BD Biosciences) according to the manufacturer's instructions and were read with an Axioplan2 imaging microscope (Carl Zeiss) and interpreted using KS Version 4.5.21 software (Carl Zeiss).

Immunofluorescence and confocal microscopy image acquisition

Immunofluorescent labeling was performed as previously described (22). The NK-sensitive targets (K562 erythroleukemia cell line and primary AML blasts) were labeled with CellTracker Blue CMAC (Molecular Probes). NK cell/target cell conjugates were formed by suspending equal volumes and cell numbers of NK effector cells (5×10^6/ml) and target cells (class I deficient K562 cells or AML blasts) in culture medium for 15 min at 37°C. Cells were transferred onto microscope slides using a cell concentrator and then fixed with 3% methanol-free formaldehyde and permeabilized. F-Actin was stained with Alexa-594-conjugated phalloidin (Invitrogen).

For perforin, CD2, or LFA-1 antibody co-staining with F-actin, slides were incubated for 1 h with primary antibodies followed by the addition of the Alexa Fluor 488 dye-conjugated goat anti-rabbit secondary antibody. The primary antibodies used were specific for perforin (delta 9, PharMingen), CD2 (RPA-2.10, BD Biosciences), LFA-1 (WT1, BD Biosciences), and high-affinity LFA-1 (MHM24, which specifically recognizes the high-affinity or "active" conformation state of LFA-1 on NK cells). Images were acquired using an Olympus IX-81 microscope equipped with DSU attachment, which utilizes a mercury arc lamp and filter cubes. Analysis was performed using the Slide Book software (Intelligent Imaging Innovations). Slides were scanned using Nomarski optics, and conjugates were identified as NK cells (small cells) and K562 cells (large cells, stained blue) or human AML blasts (large cells, stained blue) that were in obvious contact using bright field differential interference contrast (DIC). Image sets to be compared were acquired during the same session and using the same acquisition settings.

Quantitative image analysis of conjugate formation and F-actin polymerization

Quantification of F-actin, CD2, LFA-1, and perforin at the immune synapse was based on previously described methods, including independent scoring of at least 50 randomly selected conjugates per experiment using NK cells clearly contacting K562 or AML blast cells (stained blue). Those conjugates showing a distinct polymerized protein band at the NK cell:target cell contact site were considered polarized (score = 1). In addition, conjugates lacking protein polymerization (score = 0) or showing weak polymerization (score = 0.5) were included in this analysis. All polarization results were verified using ImageJ quantitative algorithm software (multi-measure plugin) to calculate the relative recruitment index (RRI) of proteins to the NK cell synapse site as previously described (22). The RRI was calculated as (mean fluorescence intensity (MFI) at NK cell synapse – background)/ (MFI at the NK cell regions not in contact with target cells – background).

Transplantation of human AML cells into NOD-SCID-IL-2Rg^{null} mice and treatment with CB-NK cells

NOD-SCID-IL-2Rg^{null} mice were bred and housed at M. D. Anderson Cancer Center. Mice were sublethally irradiated with 3 Gy before intravenous injection of 10^7 human AML cells per mouse. Human leukemia engraftment was evaluated by flow cytometric analysis of peripheral blood, spleen, and bone marrow. Human AML stem cells from two different patients were infused into 12 primary NOD-SCID-IL-2Rg^{null} mice per patient sample (10×10^6 AML cells per mouse). Once the AML cells engrafted, bone marrow harvested and infused into secondary mice (2×10^6 marrow cells per mouse). Seven days later, six of the 12 mice per experiment received the expanded NK cells (of 5×10^6 per mouse), while the other six received saline as controls. The mice were then assayed weekly for 12 weeks for the percent of AML cells detected in the blood as previously described (23).

NK cell adhesion assay

LFA-1-mediated adhesion to immobilized ICAM-1 was via assays as described previously (24). Briefly, Immunolon HB 96-well plates (Thermo-Scientific) were coated with recombinant 10 mg /ml human ICAM (Millipore), or 10 mg /ml BSA as control in PBS overnight at 4^{o}C. The plates were washed and then blocked with 1 mg/ml BSA at 37^{o}C for 2 h. CB-NK cells were plated in triplicate at 1×10^5 per well, incubated for 1 h at 37°C, and then washed with PBS three times. NK cells remaining in each well were counted using a hemacytometer. The percentage of cells that adhered to BSA-coated wells was used as control for nonspecific binding. The percentage of adhesion was then calculated.

mAb blocking experiments

For blocking experiments, IL-2 activated CB-NK cells were preincubated with 10 ng/ml anti-CD2 mAb, with anti-LFA-1 mAb (clone MHM24) or with both at 37°C for 30 min; IgG and no antibody-treated CB-NK cells were used as control. These treated cells were then washed and subsequently conjugated with labeled AML blasts for synapse studies or used in cytotoxicity assays.

Statistical analysis

For the synapse assay, statistical analyses between experimental groups were performed to evaluate the differences in the relative recruitment index (RRI) using the nonparametric Mann-Whitney test using PRISM software. For the ELIPOT and chromium release assays, as well as the antibody blocking and animal experiments, statistical analyses were performed using the two-tailed Student's *t* test.

Results

Ex vivo IL-2 expansion of CB-NK cells preserves NCRs and KIR receptors

To investigate the cellular mechanism of CB-NK functional impairment, we isolated unmanipulated NK cells from CB by $CD56^+$ selection. In addition, we wished to establish an *ex vivo* expansion method using IL-2 that could repair CB-NK cell function for comparison with the unexpanded cells. PB-NK cells were included in this study as a positive control for functional analysis. Immunophenotyping before expansion demonstrated the presence of a large population of $CD56^+CD16^-CD3^-$ CB-NK cells (mean 44.3 ± 10% SEM from 6 independent cell preparations, 47.3% in Fig. 1*A*). IL-2 expansion promoted CD16 receptor expression with the presence of a predominantly $CD56^+CD16^+CD3^-$ subset of CB-NK cells (mean 70 ± 14% from 6 independent cell preparations, 64% in Fig. 1*A*). CB-NK cells expanded an average of 92 fold (range 39 to 112 fold, n = 10 expansions) in 14 days. Similarly, PB-NK-cells expanded 83 fold (range 32 to 96 fold, n = 10 expansions) in 14 days (Supplementary Figure 1A). The results show that expansion promotes a CB-NK subset of cells that is $CD56^+CD16^+$ similar to expanded PB-NK cells (Fig. 1*A*).

We next analyzed the surface expression of the activating NCR NKp30, NKp46, and NKp44 on CB-NK cells before and after expansion compared with PB-NK cells. Both NKp30 and NKp46 were highly expressed on freshly isolated CB-NK cells, whereas NKp44 was only expressed after *ex vivo* IL-2 expansion (Fig. 1*B-D*). $CD56^+NKp44^+$ CB-NK cells increased gradually during the course of IL-2 driven expansion with maximal numbers achieved at day 14 (Supplementary Figure 1B). Similar results were also observed for PB-NK cells.

We then assessed whether the KIR repertoire of CB-NK cells was preserved before and after expansion. Unmanipulated CB-NK and PB-NK cells revealed a heterogeneous population that expressed KIR2DL1 (CD158a) and KIR2DL1/DL3/DS2 (CD158b). All NK cells

expressed the inhibitory receptor CD94-NKG2A. Of note, *ex vivo* IL-2 expansion did not change the KIR expression level on CB- or PB-NK cells (Fig. 1*E*).

In addition, we analyzed CD27 and CD11b expression on CB-NK cells pre- and post- IL-2 expansion (Supplementary Figure 1C). The majority of unexpanded CB-NK cells were $CD56^{dim}$ (over 97%) and $CD27^{+}CD11b^{+}$. After IL-2 expansion, we observed that both $CD56^{bright}$ and $CD56^{dim}$ CB-NK cell populations were uniformly $CD27^{-}CD11b^{+}$. As $CD27^{-}$ NK cell subsets are associated with strong lytic function this data suggested that our IL-2 expansion protocol induced a CB-NK lytic phenotype.

Unlike freshly isolated CB-NK cells, IL-2-expanded CB-NK cells exhibit cytolytic activity against leukemia target cells

The cytolytic functions of freshly isolated CB-NK cells and IL-2-expanded CB-NK cells were then compared with those of PB-NK cells. Freshly isolated CB-NK cells had markedly reduced cytolytic activity against MHC class I deficient K562 cells and primary patient AML blasts compared with PB-NK cells (Fig. 2*A* and *B*). In contrast, after IL-2 expansion, both CB-NK and PB-NK cells demonstrated similar levels of cytolytic activity against K562 and AML targets (Fig. 2*A* and *B*). In addition, expanded CB- and PB-NK cells showed comparable enhanced killing of AML blasts treated with an HLA class I blocking antibody (data not shown). The human B-lymphoblastoid cell line Daudi was used as a negative control for all cytotoxicity experiments as it is not susceptible to NK lysis. Expanded CB-NK cells also exhibited significantly increased frequency of IFN-γ secretion compared with unmanipulated NK cells ($p < 0.001$), although less than shown by expanded PB-NK cells ($p < 0.01$) (Fig. 2*C*). Taken together, these data suggest that *ex vivo* IL-2 expansion promotes CB-NK cells capable of killing leukemia target cells that are comparable in function to PB-NK cells.

CB-NK cells exhibit impaired F-actin immune synapse formation that can be reversed with ex vivo IL-2 expansion

We hypothesized that unmanipulated CB-NK cells would exhibit impaired formation of the immunological synapse known to translate tightly regulated signaling into appropriate NK cell functional responses to leukemia target cells. F-actin polymerization is a hallmark of the activated NK lytic synapse, whereas the inhibitory immune synapse in NK cells is predominately actin-independent (16). Thus, we focused our studies on examining F-actin polarization following NK cell-target conjugate interactions using confocal microscopy. Our initial observation was that the frequency of unexpanded CB-NK cells to form conjugates (33 ± 7%) was suppressed compared with IL-2-expanded CB-NK cells (85 ± 4%).

In subsequent experiments, freshly isolated CB-NK cells exhibited impaired F-actin synapse formation with both K562 and AML target cells compared with PB-NK cells ($p < 0.001$) (Fig. 3*A* and 3*B*). In comparison, IL-2 expansion of CB-NK cells significantly enhanced the formation of the NK immune synapse ($p < 0.001$) in both K562 and AML blast conjugates to levels comparable to those of PB-NK cells (Fig. 3*A* and *B*). These data identify a cellular mechanism for impaired CB-NK cytotoxic function and demonstrate reversal of this defect with IL-2 by the improved cytolytic killing of expanded CB-NK cells (Fig. 2*A* and *B*).

Ex vivo IL-2 expansion enhances recruitment of CD2 and LFA-1 to CB-NK cell synapses

CD2 and LFA-1 are key receptors thought to promote firm NK cell and target cell interactions as well as inducing critical downstream activation signaling during the initiation phase of lytic synapse formation (19). Because freshly isolated CB-NK have poor cytolytic activity, we hypothesized that the recruitment of the CD2 and LFA-1 signaling molecules to the synapse site might be less effective in freshly isolated CB-NK cells. We firstly

determined expression levels of CD2 and LFA-1 on freshly isolated CB-NK cells compared with *ex vivo* IL-2-expanded CB-NK cells. As shown in Fig. 4*A*, we observed a heterogeneous CD2-expressing population in unmanipulated CB-NK cells. Unexpanded CB-NK cells had predominately intracellular, non-polarized CD2 expression from confocal image analysis (data not shown). However, IL-2 expansion promoted increased CD2 expression on CB-NK cells (Fig. 4*A*). Freshly isolated CB-NK cells expressed high levels of LFA-1 that increased following IL-2 expansion (Fig. 4*B, C*). Additionally, IL-2 expansion resulted in activation of LFA-1 as measured by an antibody (clone MHM24) specific for the high-affinity conformation of LFA-1 (Fig. 4*C*). In contrast, PB-NK cells expressed increased levels of both CD2 and LFA-1 compared with unexpanded CB-NK cells, but levels were comparable to those expressed by IL-2-expanded CB-NK cells (data not shown).

We next measured recruitment of CD2 and LFA-1 to the contact site and compared unmanipulated CB-NK versus expanded CB-NK cell interactions with target cells. IL-2 expansion promoted a significant increase in the polarization of both high-affinity LFA-1 (detected using antibody clone MHM24) and CD2 receptors to the CBNK cell synapse, compared with unexpanded cells ($p < 0.001$) (Fig. 4*D-G*). Enhanced recruitment of both receptors in CB-NK cells was similar to that in PB-NK cells, consistent with comparable synapse formation (Fig. 4*F-I*). Taken together, these data suggest that IL-2 promotes the formation of the activating NK cell immunological synapse by enhancing key receptor clustering and activity at the CB-NK:target cell contact site.

Both LFA-1 and CD2 play an important role in expanded CB-NK function

We further examined the role of CD2 and LFA-1 in expanded CB-NK lytic synapse function. As shown in Fig. 5*A-C*, blockade of the individual receptors using specific blocking mAbs significantly reduced both F-actin synapse formation and the cytolytic activity of the expanded CB-NK cells ($p < 0.01$). However, the combination of CD2 and LFA1 mAbs resulted in profound inhibition of synapse formation and lytic activity ($p < 0.05$), compared with treatment with either mAb alone and mirrored the impaired function of unexpanded CB-NK cells (Fig. 5*B* and *C*). Hence, these results demonstrate that IL-2 enhancement of CB-NK cell lytic synapse function depends on the successful recruitment and activity of both CD2 and LFA-1.

LFA-1 binding to its ligand ICAM-1 on the target cells is known to be an important early event in NK cell recognition of a cell target. We therefore examined adhesion of CB-NK cells to immobilized ICAM-1 and identified a significantly reduced percentage of adherent unexpanded CB-NK cells compared with IL-2-expanded CB-NK cells ($p <0.001$) (Fig. 5*D* and *E*). This impaired adhesion is in agreement with our earlier observation that unexpanded CB-NK cells exhibit reduced conjugate formation with target cells. Moreover, enhanced LFA-1 adhesion activity with IL-2 expansion is in keeping with our observation that IL-2-expanded CB-NK cells express increased high-affinity LFA-1 compared with unmanipulated CB-NK cells (Fig 4*C*).

Ex vivo IL-2 expansion promotes polarization of perforin to CB-NK lytic immunological synapses

LFA-1 engagement by ICAM-1 is known to induce cytolytic granule polarization toward target cells. This polarization of perforin-rich lytic granules is a critical requirement for the effector function of the NK-cell lytic synapse. We initially evaluated total intracellular levels of perforin in non-conjugated CB-NK cells using confocal microscopy. Unexpanded CB-NK cells exhibited levels of perforin expression comparable to those seen in expanded CB-NK cells and PB-NK cells (Fig. 6*A*). Next we examined the recruitment of perforin to the NK cell:target cell contact site. Unexpanded CB-NK cells showed very low levels of perforin

polarization to the contact site compared with PB-NK cells, an observation in keeping with the poor cytolytic activity of the unmanipulated CB-NK cells (Fig. 2*A* and *B*). IL-2 expansion, however, significantly increased recruitment of perforin to the CB-NK cell synapse compared with unexpanded cells ($p < 0.001$) (Fig. 6*B*). As shown in Fig. 6*B*, this enhanced polarization of perforin to the contact site was similar to that in PB-NK cells and was consistent with repaired cytolytic effector function (Fig. 2*A* and *B*). Hence, these results demonstrate that following IL-2 expansion and contact with a target cell, the *ex vivo* manipulated CB-NK cells show enhanced recruitment of perforin to the mature CB-NK effector synapse.

Engraftment of human AML is inhibited after adoptive transfer of IL-2-expanded CB-NK cells in NOD-SCID-IL-2Rg^{null} mice

Previous studies have demonstrated effective anti-leukemic activity of infused PB-NK cells in murine models of AML (25). We therefore aimed to evaluate the function of expanded CB-NK cells in a human AML xenograft model using NOD-SCID-IL-2Rg^{null} mice. The grafts generated in these mice after transplantation of human primary AML cells were leukemic and of myeloid lineage (Supplementary Figure 2). The engraftment level of AML cells in the primary recipient bone marrow ranged from 15% to 70% at 8-12 weeks. The bone marrow from the primary mice that achieved 70% engraftment of AML was then harvested and injected into the tail vein of secondary mice as depicted in Fig 7*A*. IL-2-expanded CB-NK cells were then infused into these secondary mice. These experiments showed that the leukemia burden of mice infused with a single dose of 5×10^6 expanded CB-NK cells was markedly decreased in comparison to the untreated group during the 12-week observation period. Specifically, IL-2-*expanded* CB-NK-treated mice were leukemia free for up to 5 weeks and had a lower leukemia burden at 6-12 weeks compared with mice that were treated with saline only (Fig. 7*B* and *C*, $p < 0.05$). These results demonstrate *in vivo* anti-leukemic activity of adoptively transferred IL-2-expanded CB-NK cells for the first time.

Discussion

Autologous NK cell dysfunction has been correlated with poor survival in AML patients (26). In this study we wanted to determine whether allogeneic NK cells could be generated from CB for post-transplant adoptive therapy. However, the impaired cytolytic ability typically exhibited by CB-NK cells currently poses a potential obstacle for exploiting their anti-tumor potential (13). Thus, identifying the nature of CB-NK cell functional impairment should facilitate the use of CB for adoptive NK cell therapy. In this study, we expanded CB-NK cells using a GMP-compliant, IL-2-based expansion approach similar to strategies used to expand PB-NK cells for clinical use (27). Furthermore, we characterized the cellular mechanism of CB-NK cell impairment and generated functional CB-NK cells for potential clinical use.

The effector function of NK cells is tightly regulated by balancing opposing activating receptor and MHC class I inhibitory receptor signaling, including KIRs. Interaction of KIRs with self-MHC class I ligands expressed on target cells negatively regulates NK cell activity. Conversely, the absence of an inhibitory signal allows interaction of activation receptors with their ligands. Here, we show that despite expressing a comparable repertoire of KIRs and activation receptors, unmanipulated CB-NK cells are impaired in their ability to kill MHC class I deficient K562 cells in comparison to unexpanded or expanded PB-NK cells. Hence, the absence of MHC class I expression on target cells is not sufficient to activate freshly isolated CB-NK cells.

Importantly we demonstrate that IL-2 expansion of CB-NK cells *ex vivo* can induce lytic function against target cells, including MHC class I deficient K562 cells and primary AML blasts. IL-2 expansion of CB-NK cells resulted in a predominantly $CD16^{+}CD56^{+}CD27^{-}CD3^{-}$, phenotype, with gradual increase in NKp44 receptor expression. Moreover, IL-2 expansion did not alter KIR or activation receptor expression in comparison with unmanipulated CB-NK cells or PB-NK cells. These findings led us to hypothesize that freshly isolated CB-NK cells have not yet activated a cellular mechanism controlling effector function. Our results demonstrate that unmanipulated CB-NK cells have an impaired ability to form conjugates and F-actin immunological synapses with target cells compared to PB-NK cells. IL-2 expansion reverses this impairment allowing enhanced NK cell lytic synapse formation and killing of leukemia target cells.

The interaction between the NK cells and susceptible target cells (e.g., tumor cell) results in the formation of the activating NK cell immunological synapse. The formation of this lytic synapse involves several phases including: (i) adhesive contact, (ii) receptor and F-actin polarization and signaling, and (iii) directed secretion of lytic-granule contents for target killing. We further investigated the mechanism of IL-2 CB-NK cell functional activation by examining the expression and recruitment of early regulators of lytic synapse function. Activation of LFA-1 is critical for the initiation and activation stages of NK-cell lytic synapse formation, as evidenced by congenital diseases such leukocyte adhesion deficiency type I (LAD-1) in which the inherent defect in LFA-1 leads to decreased NK cell synapse formation with targets cells and reduced cytolytic function. (28). LFA-1 has been shown to control later signals for lytic granule polarization including organization and vesicular traffic at cytotoxic synapses (29, 30). *Ex vivo* IL-2 expansion of CB-NK cells increased the surface expression of both CD2 and the β2 integrin LFA-1 and increased LFA-1 mediated adhesion to ICAM-1 comparable to PB-NK cells. NK cell integrin adhesion has also been shown to be up-regulated by a number of activating receptors including CD2 (17). The increased surface expression of CD2 on CB-NK cells after IL-2 expansion may therefore play a role in regulating integrin clustering and the high-avidity state required for NK cell activation. Critically, IL-2 expansion promoted recruitment and polarization of these receptors to the CB-NK:target cell contact site. Furthermore, in blocking experiments we identified an additive role of CD2 and LFA-1 in the enhanced synapse formation and cytolytic function of expanded CB-NK cells. Our data suggests that IL-2 expansion of CB-NK cells activates F-actin immunological synapse signaling in response to target cells including CD2 and LFA-1 recruitment and activity, and perforin polarization to the mature lytic synapse.

Lastly, we demonstrated the anti-leukemic function of IL-2-expanded CB-NK cells using the NOD/SCID/IL-$2Rg^{null}$ murine model. In this model, deficiency of the IL-2 receptor γ-chain blocks not only T and B cell development but NK cell development as well (31). (32-34). This model is therefore ideal for evaluating the anti-leukemic function of infused CB-NK cells *in vivo*. Our results showed that infusion of a single dose of IL-2-expanded CB-NK cells could eliminate leukemia in these mice for up to 5 weeks, comparable to the efficacy of PB-NK cells in the NOD-SCID model (25).

In summary, we have identified that CB-NK cells exhibit impaired F-actin immune synapse formation that prevents cytolytic activity. This suppressed cellular mechanism can be activated with *ex vivo* IL-2 expansion that allows recruitment and activity of key regulators involved in CB-NK cell lytic synapse formation, enabling effective killing of leukemic cells *in vitro* and *in vivo*. Adoptive transfer of IL-2-expanded CB-NK cells may therefore provide a promising new paradigm for the treatment of minimal residual disease in patients with AML and other hematological malignancies after cord blood transplantation.

Supplementary Material

Refer to Web version on PubMed Central for supplementary material.

Acknowledgments

This work was supported by the Global CLL Global Research Foundation (JGG, EJS, CMB), NCI RO1 CA061508-16 (EJS) and the Dan L Duncan Baylor College of Medicine-M. D. Anderson Cancer Center Developmental MRP Award (CMB, EJS). We are very grateful for the helpful discussions with Jordan S. Orange and Lewis L Lanier and would also like to thank Dr. Qing Ma's laboratory for the LFA-1 monoclonal antibody clone MHM24.

Abbreviations used in this article

CB	cord blood
NCR	natural cytotoxicity receptor
IS	immune synapse
KIR	killer cell Ig-like receptor
NOD-SCID-IL-2Rg^{null}	non-obese diabetic severe combined immunodeficient interleukin-2 receptor common gamma chain null mouse model
F-actin	filamentous actin
LFA-1	leukocyte function-associated antigen-1 (CD11a-CD18 or αLβ2)

REFERENCES

1. Caligiuri MA. Human natural killer cells. Blood. 2008; 112:461–469. [PubMed: 18650461]
2. Trinchieri G. Biology of natural killer cells. Adv Immunol. 1989; 47:187–376. [PubMed: 2683611]
3. Morel E, Bellon T. HLA class I molecules regulate IFN-gamma production induced in NK cells by target cells, viral products, or immature dendritic cells through the inhibitory receptor ILT2/CD85j. J Immunol. 2008; 181:2368–2381. [PubMed: 18684926]
4. Lanier LL. Missing self, NK cells, and *The White Album*. J. Immunol. 2005; 174:6565. [PubMed: 15905491]
5. Lanier LL. NK cell recognition. Annu Rev Immunol. 2005; 23:225–274. [PubMed: 15771571]
6. Valiante NM, Uhrberg M, Shilling HG, et al. Functionally and structurally distinct NK cell receptor repertoires in the peripheral blood of two human donors. Immunity. 1997; 7:739–751. [PubMed: 9430220]
7. Vitale M, Bottino C, Sivori S, et al. NKp44, a novel triggering surface molecule specifically expressed by activated natural killer cells, is involved in non-major histocompatibility complex-restricted tumor cell lysis. J Exp Med. 1998; 187:2065–2072. [PubMed: 9625766]
8. Hsu KC, Keever-Taylor CA, Wilton A, et al. Improved outcome in HLA-identical sibling hematopoietic stem-cell transplantation for acute myelogenous leukemia predicted by KIR and HLA genotypes. Blood. 2005; 105:4878–4884. [PubMed: 15731175]
9. Passweg JR, Stern M, Koehl U, et al. Use of natural killer cells in hematopoetic stem cell transplantation. Bone Marrow Transplant. 2005; 35:637–643. [PubMed: 15654351]
10. Miller JS, Soignier Y, Panoskaltsis-Mortari A, et al. Successful adoptive transfer and in vivo expansion of human haploidentical NK cells in patients with cancer. Blood. 2005; 105:3051–3057. [PubMed: 15632206]
11. Rocha V, Labopin M, Sanz G, et al. Transplants of umbilical-cord blood or bone marrow from unrelated donors in adults with acute leukemia. N Engl J Med. 2004; 351:2276–2285. [PubMed: 15564544]

12. Willemze R, Rodrigues CA, Labopin M, et al. KIR-ligand incompatibility in the graft-versus-host direction improves outcomes after umbilical cord blood transplantation for acute leukemia. Leukemia. 2009; 23:492–500. [PubMed: 19151783]
13. Dalle JH, Menezes J, Wagner E, et al. Characterization of cord blood natural killer cells: implications for transplantation and neonatal infections. Pediatr Res. 2005; 57:649–655. [PubMed: 15718362]
14. Gaddy J, Broxmeyer HE. Cord blood CD16+56- cells with low lytic activity are possible precursors of mature natural killer cells. Cell Immunol. 1997; 180:132–142. [PubMed: 9341743]
15. Stinchcombe JC, Bossi G, Booth S, et al. The immunological synapse of CTL contains a secretory domain and membrane bridges. Immunity. 2001; 15:751–761. [PubMed: 11728337]
16. Orange JS. Formation and function of the lytic NK-cell immunological synapse. Nat Rev Immunol. 2008; 8:713–725. [PubMed: 19172692]
17. Inoue H, Miyaji M, Kosugi A, et al. Lipid rafts as the signaling scaffold for NK cell activation: tyrosine phosphorylation and association of LAT with phosphatidylinositol 3-kinase and phospholipase C-gamma following CD2 stimulation. Eur J Immunol. 2002; 32:2188–2198. [PubMed: 12209631]
18. Mace EM, Monkley SJ, Critchley DR, et al. A dual role for talin in NK cell cytotoxicity: activation of LFA-1-mediated cell adhesion and polarization of NK cells. J Immunol. 2009; 182:948–956. [PubMed: 19124737]
19. Chen XP, Trivedi BG, Krzewski K, et al. Many NK cell receptors activate ERK2 and JNK1 to trigger microtubule organizing center and granule polarization and cytotoxicity. Proc.Natl.Acad.Sci.U.S.A. 2007; 104:6329–6334. [PubMed: 17395718]
20. Carpen O, Virtanen I, Saksela E. Ultrastructure of human natural killer cells: nature of the cytolytic contacts in relation to cellular secretion. J Immunol. 1982; 128:2691–2697. [PubMed: 7077081]
21. Wulfing C, Purtic B, Klem J, et al. Stepwise cytoskeletal polarization as a series of checkpoints in innate but not adaptive cytolytic killing. Proc Natl Acad Sci U S A. 2003; 100:7767–7772. [PubMed: 12802007]
22. Ramsay AG, Johnson AJ, Lee AM, et al. Chronic lymphocytic leukemia T cells show impaired immunological synapse formation that can be reversed with an immunomodulating drug. J Clin Invest. 2008; 118:2427–2437. [PubMed: 18551193]
23. Lapidot T, Sirard C, Vormoor J, et al. A cell initiating human acute myeloid leukaemia after transplantation into SCID mice. Nature. 1994; 367:645–648. [PubMed: 7509044]
24. Neeson PJ, Thurlow PJ, Jamieson GP. Characterization of activated lymphocyte-tumor cell adhesion. J Leukoc Biol. 2000; 67:847–855. [PubMed: 10857858]
25. Ruggeri L, Capanni M, Urbani E, et al. Effectiveness of donor natural killer cell alloreactivity in mismatched hematopoietic transplants. Science. 2002; 295:2097–2100. [PubMed: 11896281]
26. Fauriat C, Just-Landi S, Mallet F, et al. Deficient expression of NCR in NK cells from acute myeloid leukemia: Evolution during leukemia treatment and impact of leukemia cells in NCRdull phenotype induction. Blood. 2007; 109:323–3. [PubMed: 16940427]
27. Koehl U, Esser R, Zimmermann S, et al. Ex vivo expansion of highly purified NK cells for immunotherapy after haploiddentical stem cell transplantation in children Klin Padiatr. 2005; 217:345–50.
28. Krensky AM, Mentzer SJ, Clayberger C, et al. Heritable lymphocyte function-associated antigen-1 deficiency: abnormalities of cytotoxicity and proliferation associated with abnormal expression of LFA-1. J Immunol. 1985; 135:3102–3108. [PubMed: 3900204]
29. Krzewski K, Strominger JL. The killer's kiss: the many functions of NK cell immunological synapses. Curr Opin Cell Biol. 2008; 20:597–605. [PubMed: 18639449]
30. Liu D, Bryceson YT, Meckel T, et al. Integrin-dependent organization and bidirectional vesicular traffic at cytotoxic immune synapses. Immunity. 2009; 31:99–109. [PubMed: 19592272]
31. Traggiai E, Chicha L, Mazzucchelli L, et al. Development of a human adaptive immune system in cord blood cell-transplanted mice. Science. 2004; 304:104–107. [PubMed: 15064419]
32. Ito M, Hiramatsu H, Kobayashi K, et al. NOD/SCID/gamma(c)(null) mouse: an excellent recipient mouse model for engraftment of human cells. Blood. 2002; 100:3175–3182. [PubMed: 12384415]

33. Yahata T, Ando K, Nakamura Y, et al. Functional human T lymphocyte development from cord blood CD34+ cells in nonobese diabetic/Shi-scid, IL-2 receptor gamma null mice. J Immunol. 2002; 169:204–209. [PubMed: 12077246]

34. Shultz LD, Lyons BL, Burzenski LM, et al. Human lymphoid and myeloid cell development in NOD/LtSz-scid IL2R gamma null mice engrafted with mobilized human hematopoietic stem cells. J Immunol. 2005; 174:6477–6489. [PubMed: 15879151]

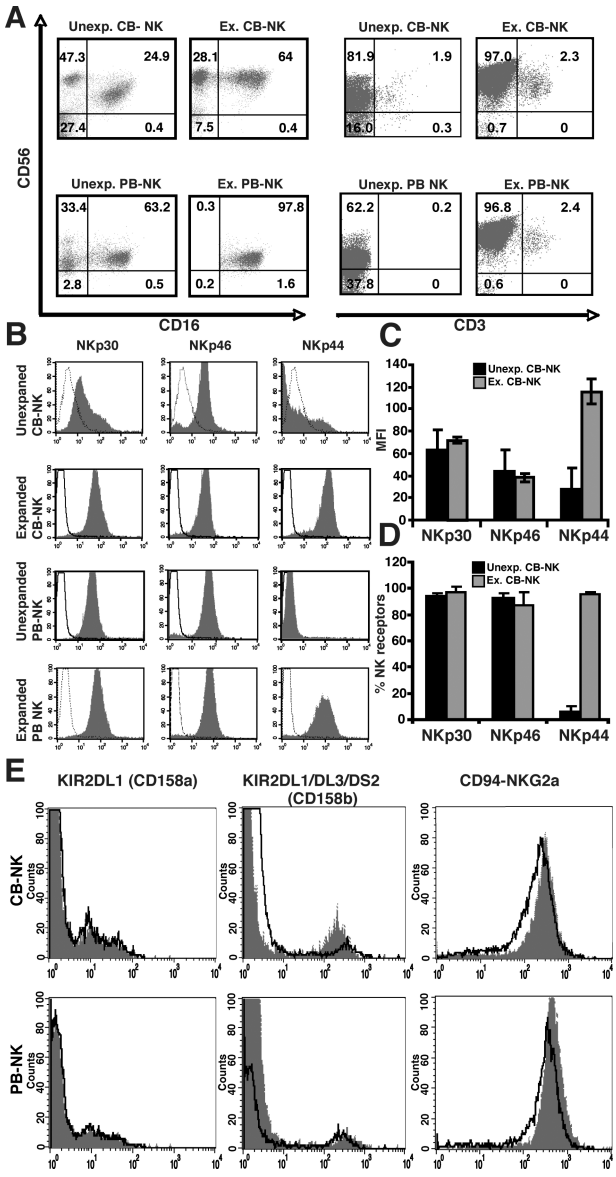

FIGURE 1.

Phenotype and NK receptor analysis of CB-NK cells and PB-NK cells before and after IL-2 expansion. *A*, Representative example (one of six) of flow cytometric analysis of unexpanded (Unexp.) compared with IL-2-expanded (Ex.) CB- and PB-NK cells. The dot plots on the left-hand side show the CD56+CD3- NK cell population. *B*, Representative flow cytometric analysis showing expression of the activating NK receptors (NCRs) NKp30, NKp46, and NKp44 on unexpanded and IL-2-expanded CB-NK and PB-NK cells. Histogram analysis was gated on the $CD56^{+}$CD3-population. Dotted lines are isotype controls, and gray-shaded histograms are receptor expression levels. *C*, Summary of the mean fluorescence intensity (MFI) of Unexp. and Ex. CB-NK cells, and *D*, percentage of receptor positive Unexp. and Ex. CB-NK cells. Values are the means ± SEM from six independent experiments. *E*, Flow cytometric analysis of killer immunoglobulin-like receptor (KIRs, CD158a and CD158b) and CD94-NKG2A expression on CB-NK and PB-NK cells before expansion (grey shaded histogram) and after expansion (black-lined

histogram overlay) from a representative CBNK and PB-NK cell line (one of six). Isotype controls were performed but are not shown.

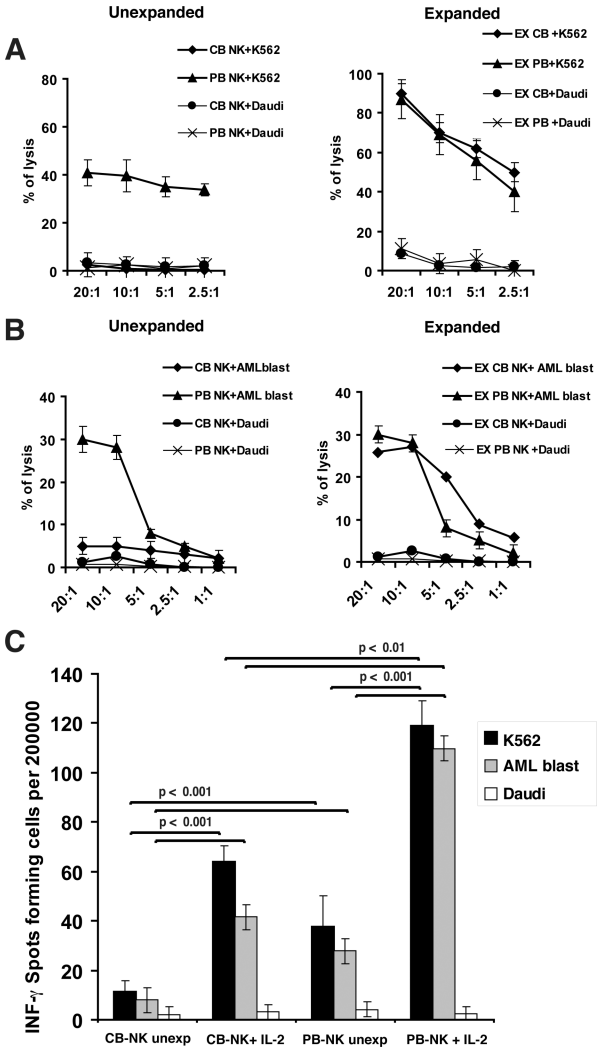

FIGURE 2.

Cytotoxic function and IFN-γ secretion of CB-NK cells compared with PB-NK cells before and after IL-2 expansion. *A* and *B* show percent specific lysis of unexpanded and IL-2-expanded CB-NK cells versus PB-NK cells. CB-NK and PB- NK cells were used in ^{51}Cr release cytotoxicity assays for 4 h against K562 cells (*A*) and AML patient primary blasts (*B*). NK cell resistant Daudi cells were used as negative control targets. *C* shows the ability of unexpanded (Unexp) and IL-2-expanded (Ex) CB-NK cells and PB-NK cells to secrete IFN-g in response to target K562 cells and primary CD33^{+} AML blasts in an IFN-g ELISPOT assay. Daudi cells were used as negative control. Values are the means ± SEM from five independent experiments.

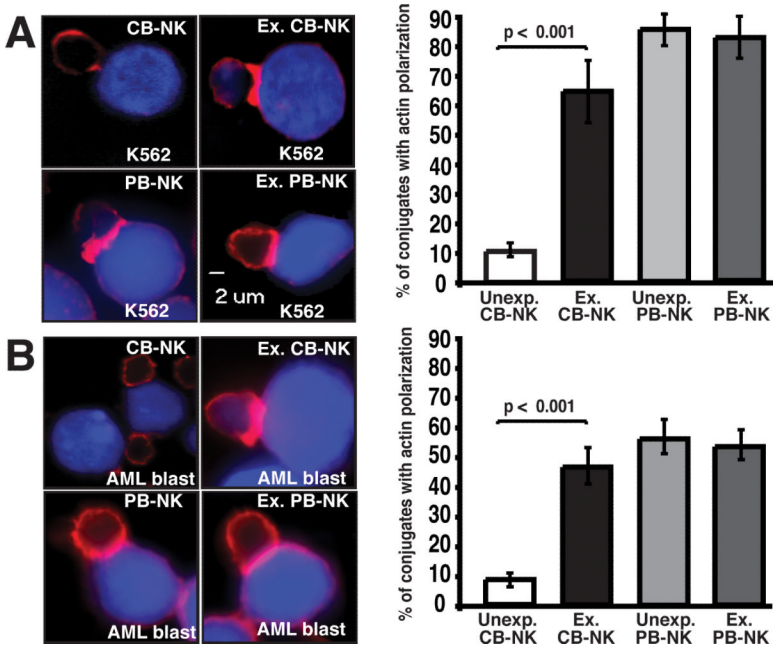

FIGURE 3.

Freshly isolated unexpanded CB-NK cells exhibit decreased immunological synapse formation that can be reversed with *ex vivo* IL-2 expansion. *A*, Left panel, confocal fluorescence microscopic images show representative examples of unexpanded and expanded (Ex.) CB- and PB-NK conjugates with K562 cells (stained blue with CMAC-dye). Images show one medial optical section in the z-plane. Original magnification 40×. The right panel shows percent of conjugates with F-actin polarization (red) corresponding to the synapse images shown on the left. *B*, Left panel, confocal fluorescence microscopic images of unexpanded and expanded (Ex.) CB- and PB-NK conjugates with AML patient primary blasts (blue). The right panel shows the percentage of F-actin accumulation at the NK immune synapse. Values are the means ± SEM from six independent experiments, with at least 50 random conjugates analyzed per experiment.

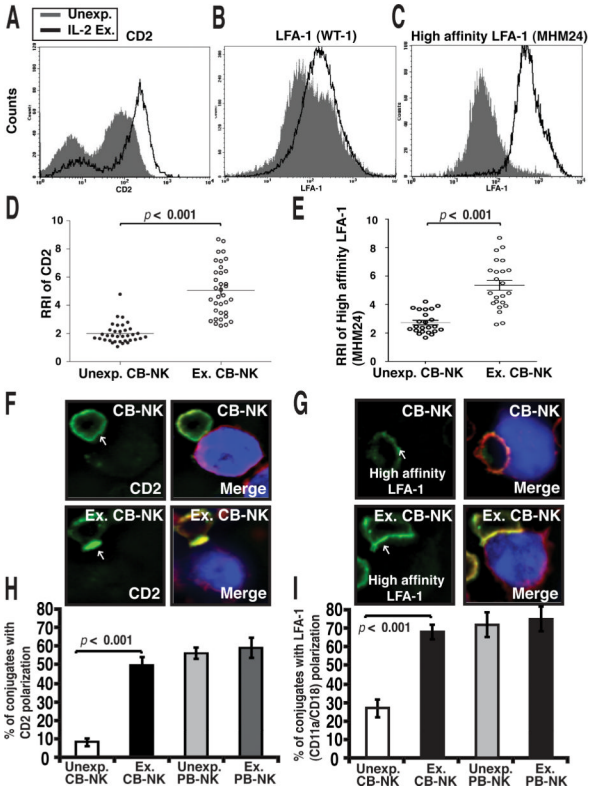

FIGURE 4.

Enhanced recruitment of CD2 and LFA-1 to CB-NK cell immune synapses following *ex vivo* IL-2 expansion. *A*, Representative flow cytometric analysis (one of six) of CD2 (*A*), LFA-1 (WT-1 mAb) (*B*), and high-affinity LFA-1 (MHM24 mAb) (*C*) expression on unexpanded (Unexp., gray-shaded histogram) compared with IL-2-expanded (Ex., black line) CB-NK cells. *D* and *E* show quantitative image analysis (relative recruitment index, RRI) of CD2 (*D*) and high-affinity LFA-1 (MHM24 mAb) (*E*) at the NK cell immunological synapse for unexpanded compared with expanded CBNK cells. Each dot represents a CB-NK cell synapse (50 conjugates analyzed per experiment). The black bar shows the mean value SEM *F* and *G*, Confocal images of CB-NK and expanded CB-NK conjugates with AML blasts (blue) stained with CD2 antibody conjugated with Alexa-488 dye (green) or the high-affinity LFA-1 antibody (MHM24) conjugated with Alexa-488 dye (green) and F-actin (red). Arrows indicate protein localization at the NK cell-AML blast synapse site. Co-localization of proteins in the merged images is shown in yellow. Original magnification 40×. *H* and *I*, Unexp. and Ex. CB-NK and PB-NK conjugates with AML blasts were scored for polarization of CD2 (*H*) or LFA-1 (*I*). Values are the means ± SEM from six independent experiments, with at least 50 random conjugates analyzed per experiment.

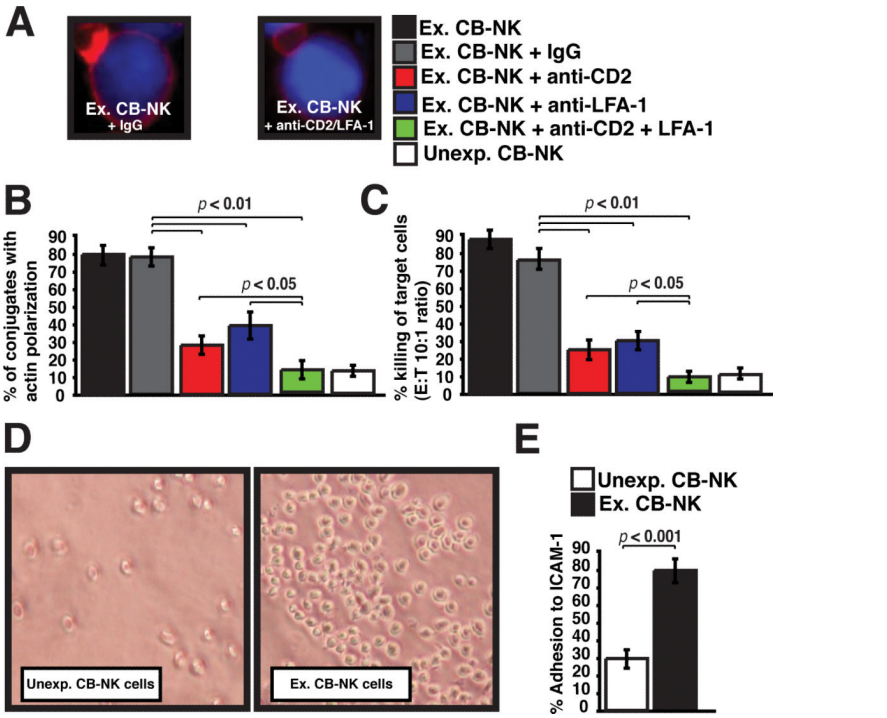

FIGURE 5.

LFA-1 and CD2 both play a critcial role in enhancing CB-NK function following IL-2 expansion. *A*, Confocal images show F-actin synapse polarization (red) of Ex CB-NK cells with AML blasts (blue) after pretreatment with IgG control blocking antibody (left image) or CD2 and LFA-1 blocking antibodies (right image). *B*, Expanded (Ex) CB-NK cells are evaluated in conjugation synapse assays (% F-actin synapse polarization) following treatment with control IgG antibody (+ IgG), CD2 blocking antibody (red bar), LFA-1 blocking antibody (blue bar), or a combination of both CD2 and LFA-1 blocking antibodies (green bar). The percentage of F-actin synapse represents six independent experiments. Error bars show the SEM. *C*, Cytolytic activity of IL-2-expanded (Ex) CB-NK cells against AML blasts was evaluated following treatment with control IgG antibody (+ IgG), CD2 blocking antibody (red bar), LFA-1 blocking antibody (blue bar), or a combination of both CD2 and LFA-1 blocking antibodies (green bar). Effector:target (ET) ratio of 10:1 is shown. Values are the means ± SEM from six independent experiments. *D,* The images show representative fields of unexpanded (Unexp) CB-NK versus expanded (Ex) CB-NK cell adherence to ICAM-1-coated plates (original magnification 10×). *E*, The percent of unexpanded (Unexp) CB-NK cells versus the percentage of expanded (Ex) CB-NK cells that adhere to ICAM-1-coated plates is shown. Values are the means ± SEM from six independent experiments.

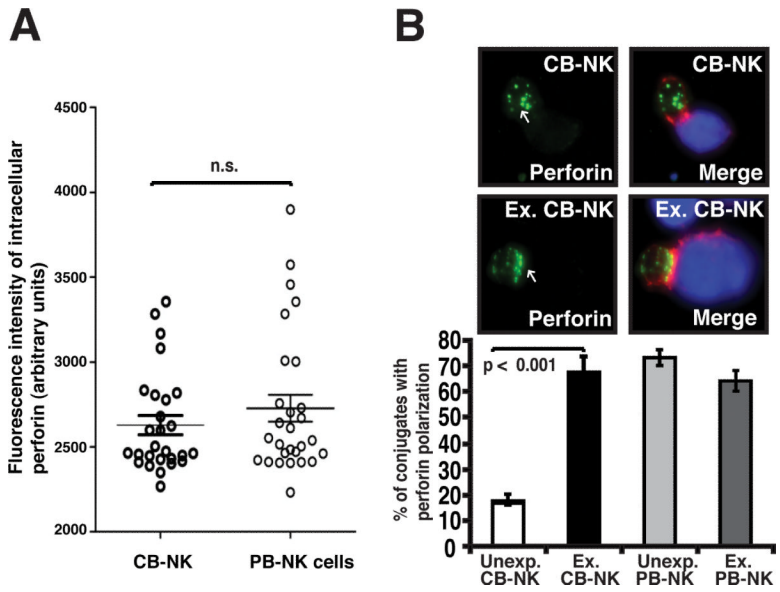

FIGURE 6.

Ex vivo IL-2 expansion of CB-NK cells promotes polarization of perforin to the lytic mature synapse. *A*, Quantitative analysis of intracellular perforin expression levels in non-conjugated CB- and PB-NK cells using confocal microscopy and image analysis is shown. Fluorescence intensity was calculated using ImageJ software. Data are representative of at least six independent experiments. Statistical analyses were performed using the nonparametric Mann-Whitney test using PRISM software. *B*, Unexp. and Ex. CB- and PB-NK conjugates with target AML blasts (stained blue) were scored for polarization of perforin (stained green) at the NK cell immune synapse (F-actin stained red). The *upper panel* shows representative confocal fluorescence microscopic images of unexpanded (Unexp.) and expanded (Ex.) CB conjugates with AML blasts. Arrows indicate protein localization at the NK cell-AML blast target cell synapse site. Co-localization of proteins in the merged images is shown in yellow. Original magnification 40×. The *lower panel* shows the percent of conjugates with perforin polarization of unexpanded and expanded CB-NK cells (corresponding to the synapse images shown in the upper panel) as well as unexpanded and expanded PB-NK cells. Values are the means ± SEM from six independent experiments, with at least 50 random conjugates analyzed per experiment.

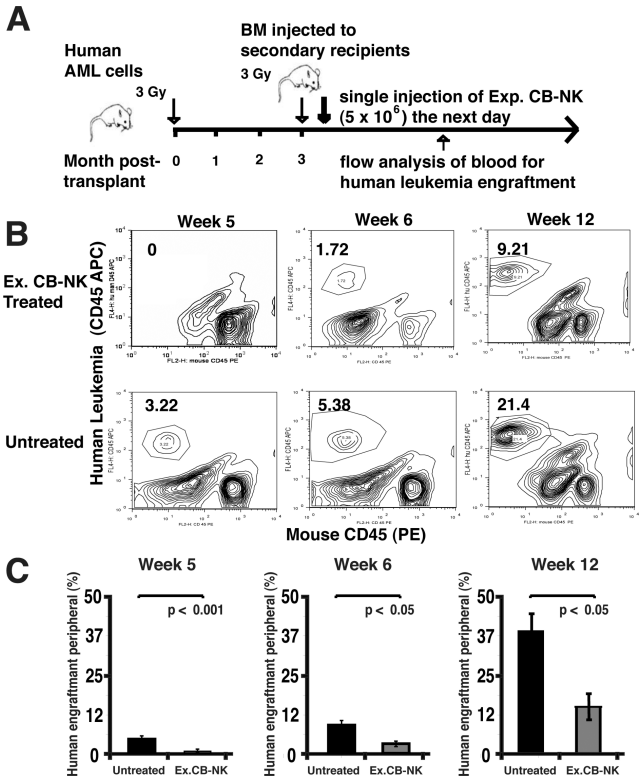

FIGURE 7.

IL-2-expanded CB-NK cells exhibit potent *in vivo* anti-leukemic effector function by inhibition of primary human AML cells engraftment in NOD-SCID-IL2Rγ^{null} mice. *A*, Schematic summary of *in vivo* functional studies using expanded CB-NK cells with a NOD-SCID-IL2Rγ^{null} model. BM, bone marrow. *B*, Representative flow cytometric analysis showing the percentage of CD45^{+} human leukemia cells detected in the peripheral blood of a control (saline treated) mouse versus a mouse treated with expanded (Ex.) CB-NK cells. Data are shown from weeks 5, 6, and 12 after CB-NK cell administration. *C*, The cumulative flow cytometric analysis of treated mice at weeks 5, 6, and 12 after infusion of IL-2 Ex. CB-NK cells compared with the control (saline treated) group is shown. Bars represent the percentage of human leukemia in the peripheral blood obtained from the control group (black bars) versus the Ex. CB-NK treated group (gray bars). Values are means ± SEM for 6 mice. Data show one of two independent studies using human AML primary cells.